Bulletin of the Seismological Society of America

This copy is for distribution only by
the authors of the article and their institutions
in accordance with the Open Access Policy of the
Seismological Society of America.

For more information see the publications section
of the SSA website at www.seismosoc.org

THE SEISMOLOGICAL SOCIETY OF AMERICA
400 Evelyn Ave., Suite 201
Albany, CA 94706-1375
(510) 525-5474; FAX (510) 525-7204
www.seismosoc.org

Bulletin of the Seismological Society of America, Vol. 100, No. 5A, pp. 2329–2337, October 2010, doi: 10.1785/0120090142

Comment on "Near-Surface Location, Geometry, and Velocities of the Santa Monica Fault Zone, Los Angeles, California" by R. D. Catchings, G. Gandhok, M. R. Goldman, D. Okaya, M. J. Rymer, and G. W. Bawden

by Thomas L. Pratt and James F. Dolan

Introduction

Catchings *et al.* (2008; hereafter referred to as Catchings *et al.*) effectively duplicated our acquisition of a high-resolution seismic reflection profile across a fault scarp near the tip of the Santa Monica fault, one of the major faults in the northern Los Angeles basin. The profiles crossed a distinct topographic scarp, which is one of a series of scarps that indicate the fault extends about 11 km across the northern Los Angeles basin before continuing undersea to the west (Dolan *et al.*, 2000). Based primarily on the seismic-reflection and refraction data, Catchings *et al.* argued that there are two active fault strands in the near surface (< 100 m depth), in contrast to the single fault that we interpreted from a combination of seismic-reflection, geomorphologic, and trench data at the same site (Dolan and Pratt, 1997; Pratt *et al.*, 1998; Dolan *et al.*, 2000). Acceptance of the interpretation of Catchings *et al.* would significantly change seismic hazard assessments in the west Los Angeles–Santa Monica area in two ways. First, the addition of a second shallow, active fault strand about 200 m south of the known fault scarp and a zone of rotated strata between the two strands, as proposed by Catchings *et al.*, would widen by ~200 m the zone of active faulting and surface deformation inferred in our earlier studies (although Catchings *et al.*, figs. 5 and 9 show fault B to reach the surface about 140 m south of the scarp, and their fig. 10 shows it to be about 100 m south of the scarp). If this same geometry were assumed along the portion of the topographic scarps for which it has not been documented, the additional zone of inferred active faulting would encompass a substantial area in this densely urbanized corridor. Second, Catchings *et al.* argue for a ~20° dip for the shallowest 700 m length of the fault, in contrast to the 55° to 70° dip interpreted by us and by Tsutsumi *et al.* (2001) for all but the shallowest tip of the fault. The shallower dip would, as pointed out by Catchings *et al.*, result in estimates of slip rates based on elevation differences at the scarp that are "significantly greater" than previous estimates using a greater fault dip. Given the potential impact on hazard assessments, we feel it is necessary to comment on several aspects of the Catchings *et al.* interpretation that we feel are unjustified or incorrect.

Background

A distinct topographic scarp is associated with the active strand of the Santa Monica fault at the southern edge of the Wadsworth Veteran's Administration Hospital (WVAH) property near downtown Santa Monica (Fig. 1; see Dolan *et al.*, 2000 for detailed discussion). This geomorphically well-defined scarp can be traced continuously for several km to the east and west of the WVAH property, except where it has been eroded by active south-flowing drainages. A trench across the scarp showed evidence for an earthquake between 10,000 and 17,000 years ago, and probably a more recent event between 1000 and 3000 years ago (Dolan *et al.*, 2000). Dolan and Pratt (1997), Pratt *et al.* (1998) and Dolan *et al.* (2000) interpreted seismic-reflection and trench data across the scarp as providing evidence that the active strand of the Santa Monica fault reaches the surface about 20 m south of the base of the topographic scarp and dips to the north beneath the trench (our summary figure is reproduced as Catchings *et al.*, fig. 9a). The trench across the scarp exposed folded late Pleistocene through late Holocene alluvial strata that are onlapped by younger (≤1000 years old) subhorizontal beds. The onlap indicates that the base of the original fold scarp, and thus the surface location of the fault, is buried beneath younger strata south of the trench (Dolan *et al.*, 2000). Similar relationships were exposed in another trench at University High School 700 m to the west of our trench site, along the same well-defined topographic scarp (Hill, 1979; Hill *et al.*, 1979). Our seismic-reflection data are consistent with the shallow part of the thrust fault dipping north at 30°–55°, although we tentatively favored the gentler dip of 30°–35° for the shallowest portion of the fault based on the presence of what could be weak footwall reflectors.

Catchings *et al.* acquired a shallow seismic-reflection profile adjacent to the trench of Dolan *et al.* (2000) that was nearly coincident with the shorter of our two profiles. In contrast to our interpretation, Catchings *et al.* proposed that the Santa Monica fault consists of two north-dipping thrust faults interpreted from what they believed to be fault-plane reflections on their seismic section (Catchings *et al.*, fig. 5). Their interpreted fault A dips northward at an angle of 28° and projects to the surface directly beneath the topographic scarp,

about 25–30 m north of where we interpreted the active fault to reach the surface (Catchings *et al.*, fig. 9). They also interpreted a deeper fault B, which they stated (page 136) is "…probably the most recently active of the thrust faults." Their fault B is interpreted to dip to the north at an angle of 20° and to reach the surface near Santa Monica Boulevard, about 200 m south of where we interpreted the thrust fault to reach the surface (Catchings *et al.*, fig. 10). They also interpreted fault B to extend north of the trench with a 20° dip for at least 700 m north of its surface projection (Catchings *et al.*, fig. 10). Catchings *et al.* argued that the slip rate on the Santa Monica fault could be "significantly greater" than past estimates, including ours, because of a lower dip angle on the active fault (their fault B) and because two faults are present. We note, however, that the dip-slip rate suggested by Dolan *et al.* (2000) for the Santa Monica fault at this site is only crudely constrained by soil age estimates, and the more-robust dip-slip rate obtained at Potrero Canyon 6 km to the west is used in current seismic hazard assessments (see Dolan *et al.* (2000) for detailed discussion).

Although we are both listed as reviewers of the Catchings *et al.* paper, we do not agree with their conclusions. We

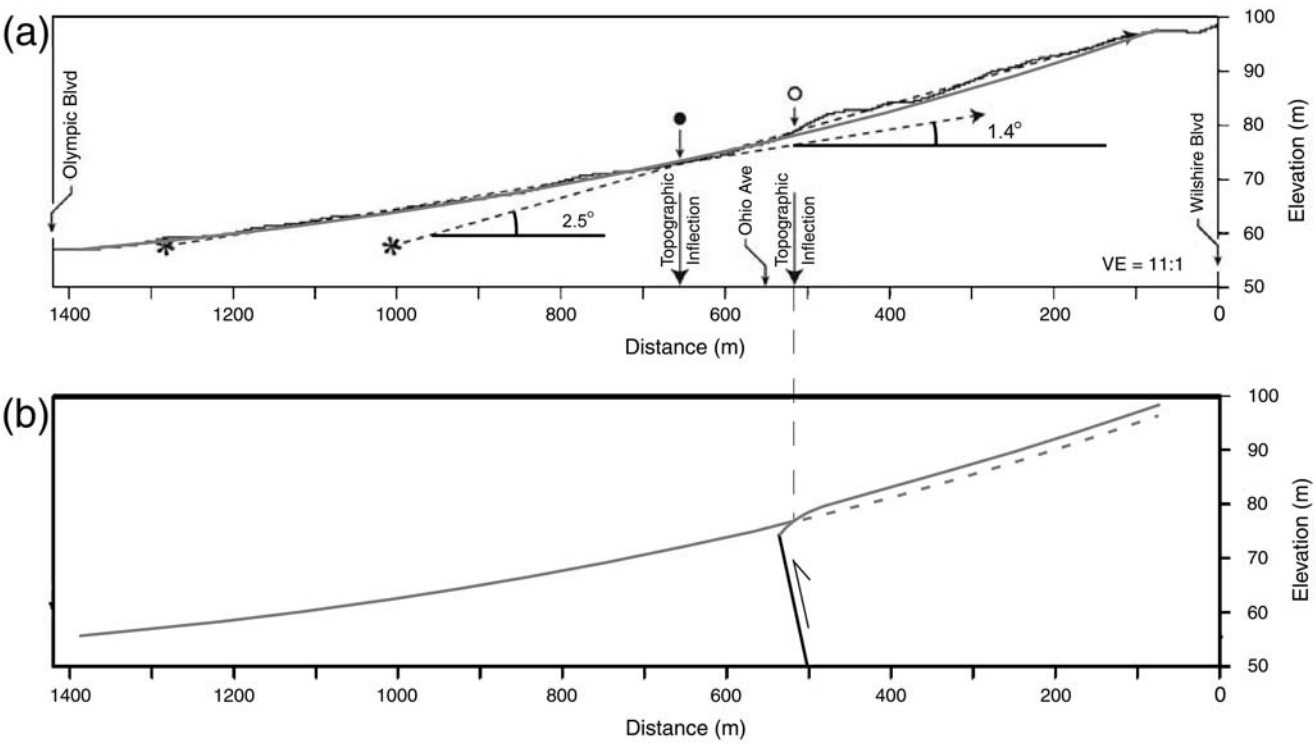

Figure 1. (a) Copy of Catchings *et al.* (2008) figure 10a, showing their north–south topographic profile across the Santa Monica fault (north is to the right). Catchings *et al.* drew two dashed, straight lines on the slope that they claimed showed an inflection with an 8° change in the dip of the slope near Santa Monica Boulevard (solid circle). The dip angles of the dashed lines according to the scales, however, are about 1.4° and 2.5° after removing the vertical exaggeration (actually about 6.5:1 rather than the 11:1 stated by Catchings *et al.*). The topographic profile can be fit almost perfectly with a mathematical model of an alluvial-fan profile based on a diffusive sediment transport model (gray line; De Chant *et al.*, 1999) except that the profile is elevated by several meters in the hanging wall north of the WVAH scarp (open circle), as would be expected due to thrust fault displacement on the active strand of the Santa Monica fault. Such concave-up profiles are typical of alluvial fans. (b) Schematic diagram showing a 35° N-dipping fault (~6.5 vertical exaggeration) cutting the topographic profile beneath Ohio Avenue and producing an uplifted hanging wall with slight folding of strata near the fault tip. Subsequent fan growth buried the lower portion of the fault scarp, giving a result similar to the observed topographic profile and consistent with the trench data. Dashed line shows the projected location of the modern surface if faulting had not occurred. Deeper portions of the fault must have a steeper dip (e.g., Dolan *et al.*, 2000). The theoretical profile is a weighted average of the two end members presented in De Chant *et al.* (1999): 40% equation (18) (homogeneous sediment deposition) and 60% equation (19) (variable sediment deposition). This average may suggest that the Sepulveda fan at Santa Monica is intermediate between the two end members, although the profile is also affected by being oblique to the slope. (c) Portion of the 1934 USGS 7.5 minute Sawtelle topographic map showing the WVAH site and areas to the south. The map was made before any significant regrading of the key area adjacent to the southern edge of Santa Monica Boulevard. The scarp just north of Ohio Avenue (labeled Ohio) is well defined as a slope on the map, with the thick dashed line with arrows showing the location of the base of the scarp. The heavy black line shows the location of the longer seismic profile of Pratt *et al.* (1998). East of the profile, the scarp has been eroded by the active Sepulveda drainage. The "S" marks the location of springs at the base of the fault scarp at University High School. The fault scarp is partially buried, so the fault nears the surface just south of the topographic scarp (Dolan *et al.*, 2000). Near Santa Monica Boulevard (labeled SMB), the alluvial-fan surface dips steadily to the south with no evidence for a topographic scarp associated with the fault B hypothesized by Catchings *et al.* (*Continued*)

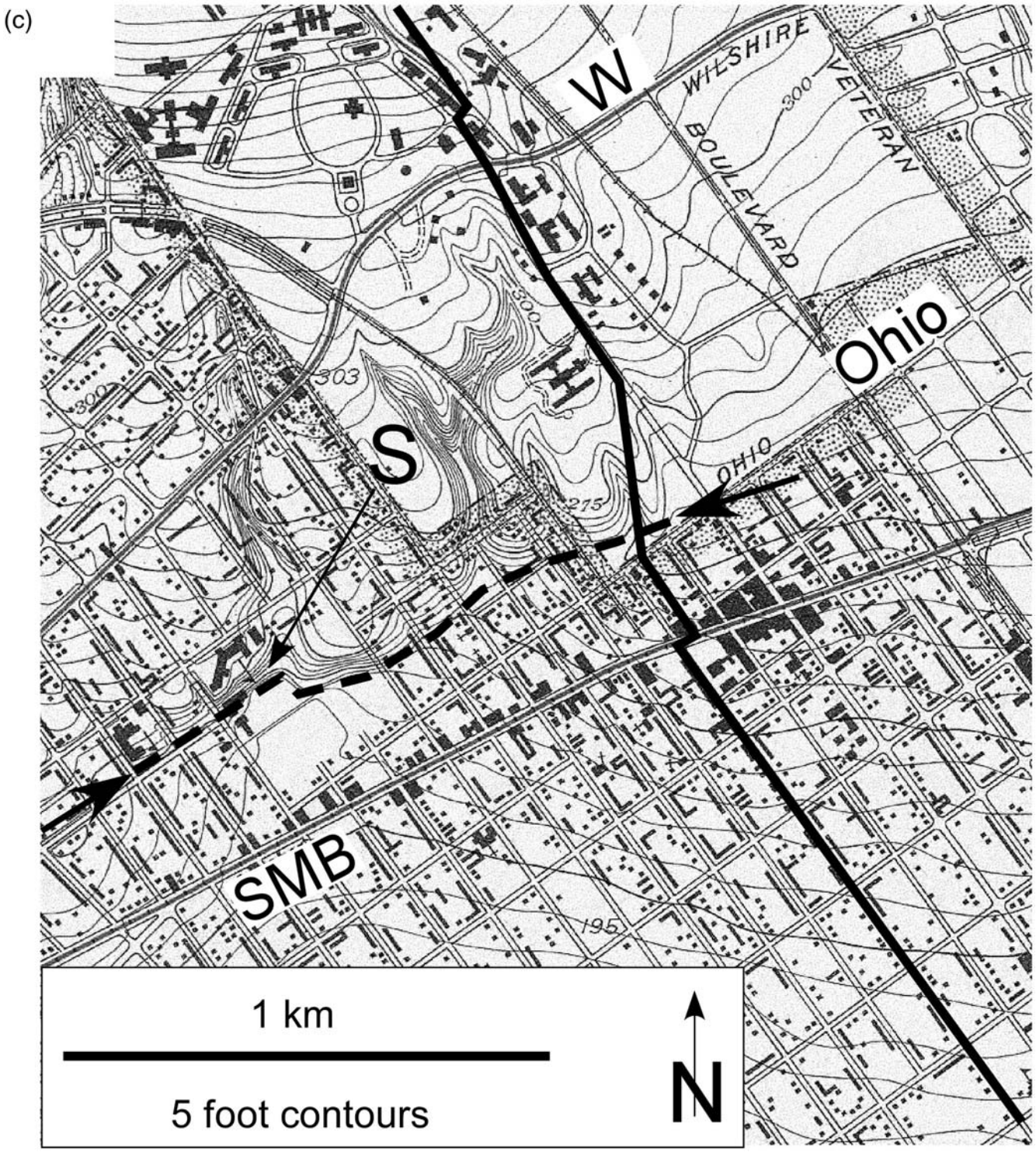

Figure 1. Continued.

made the following points in a *Bulletin of the Seismological Society of America* review that we anticipated would result in major revisions to the manuscript: (1) the interpretation by Catchings *et al.* does not honor geomorphic data that show that the fault at the trench is the only active, near-surface fault strand in the area; (2) their hypothesized deeper fault strand B has no geomorphic expression and conflicts with subsurface data; and (3) the seismic velocities they derived from their tomographic analysis and used to process the seismic-reflection data are unrealistically fast below about 25 m depth, which makes the seismic imaging suspect and likely influenced their fault interpretations.

The Active Strand of the Santa Monica Fault

We argued in our papers that the active strand of the Santa Monica fault reaches the surface just south of the base of the laterally continuous topographic scarp and WVAH trench (Dolan and Pratt, 1997; Pratt *et al.*, 1998; Dolan *et al.*, 2000), and we see nothing in the Catchings *et al.* paper to dissuade us from this conclusion. Perhaps the best evidence for the active fault on the Catchings *et al.* seismic data is the substantial change in velocity near the south end of their tomographic profile, discernible in strata as shallow as 5–10 m depth beneath the southern end of the trench (Catchings *et al.*, figs. 4 and 6). This velocity change is the first-order feature of their tomographic image and should be well defined on the seismic records by a change in the speed of the refracted arrivals. The velocity change is consistent with a thrust fault having substantial dip-slip motion and fracturing of the shallow hanging-wall strata as seen in the trench. The groundwater barrier that Catchings *et al.* mentioned is also consistent with a thrust fault having substantial slip. Indeed, the largest groundwater anomalies in the area are along the WVAH topographic scarp at University High School, several blocks west of the WVAH trench site and seismic profiles (Fig. 1). There, a series of artesian springs along the base of the fault scarp trenched by Hill (1979) and Hill *et al.* (1979) were the site of native American occupations and continue to flow. A similar groundwater barrier was noted in the foundation excavations of two buildings at the intersection of Wilshire Boulevard and Bundy Drive, 900 m west of the University High School, along the same well-defined scarp observed at the WVAH trench site (see discussion in Dolan *et al.*, 2000; p. 1565).

The thrust fault, however, must reach the surface to the south of the topographic scarp to place it at the base of the folded strata, whereas recent motion on fault A of Catchings *et al.* conflicts with direct exposures of the strata in the Dolan *et al.* (2000) trench. Specifically, the first-order structural feature exposed in the trench is a gentle (15°) south-dipping fold limb developed in alluvial-fan strata in the southernmost part of the trench. These folded beds are onlapped by younger, horizontally stratified alluvial-fan sediments that were deposited against the dipping strata. The folding and subsequent onlap of the originally near-horizontal beds within the partially buried fold scarp therefore indicate that the main active strand of the Santa Monica fault reaches the near surface just south of the trench. Faults exposed within the trench are all steeply dipping, left-lateral strike-slip and oblique reverse-sinistral faults that cut the hanging-wall fold above the main strand; the presence of these secondary strands reflects near-surface strain partitioning along the oblique-slip fault (Dolan *et al.*, 2000).

Catchings *et al.*, however, interpret their fault A to project to the surface approximately 15–20 m north of the base of the fold scarp, near the base of the topographic scarp but within the well-defined south-dipping fold limb developed above the main strand of the fault (Catchings *et al.*, fig. 9b). They state (p. 131) that there is about 10 m displacement of a shallow reflector across fault A: "…on the seismic reflection image, the reflector that correlates best with the 1500 m/sec velocity contour increases in depth from about 5 m north of fault A to about 15 m south of the surface projection of fault A." They show this distinct change in depth across fault A in the "unconsolidated sediments" in the upper 15 m of their interpretation (Catchings *et al.*, fig. 6b). It would also take substantial motion on fault A to create a fault-plane reflection. Yet there is not a thrust fault cutting the distinct paleosols near the south end of the trench (the trench was excavated specifically to look for such a fault), particularly not a thrust fault that exhibits the large vertical separation inferred by Catchings *et al.* There is also no evidence for an inflection point in the dip of the trenched strata near the surface projection of their fault A. Thus, fault A, if it exists at the position suggested by Catchings *et al.*, must be a now inactive, secondary strand within the hanging-wall of the main strand of the Santa Monica fault. The lack of deformation above the tip of their fault A is consistent with the lack of interpreted dip-slip motion on the deeper portions of their fault (see Catchings *et al.*, fig. 6b). However, a lack of recent motion on their fault A also would mean that it cannot be responsible for creating the fault scarp, thus leaving them with no explanation for the presence of the well-defined scarp. We argue that the main, active strand that folded the strata in the trench and caused an earthquake 10,000 to 17,000 years ago, and possibly 1000–3000 years ago, must lie to the south of the southernmost folded strata, at least 20 m south of the position inferred by Catchings *et al.* for their fault A. An active fault just south of the trench with folding and minor secondary hanging-wall faulting near the fault tip (e.g., our interpretation as shown in Catchings *et al.*, fig. 9a) explains the velocity change, the groundwater anomaly, the topographic scarp, and the gently folded strata in the trench. A fault in this position is not interpreted by Catchings *et al.*

Fault B

We see no evidence that hypothesized fault B, which Catchings *et al.* interpreted as the "principal near-surface trace" of the Santa Monica fault (Catchings *et al.*, pp. 129 and 136), exists as a major active, near-surface fault at the location ascribed to it by Catchings *et al.* They state (p. 136) that "…fault B is probably the most recently active of the thrust faults. Trenching studies to evaluate the recency of movement would likely be most successful in the vicinity of the surface projection of fault B, near Santa Monica Boulevard." First and foremost, there is no topographic scarp in the vicinity of Santa Monica Boulevard, where they proposed that fault B reaches the surface (Catchings *et al.*, fig. 10; see our Figure 1, with the caveats described herein). If there had been any recent thrust motion on fault strand B, which they interpret to reach the surface just north of Santa Monica Boulevard, hanging-wall strata should be uplifted

north of the fault tip to produce a step on the otherwise gently southward-sloping landscape. Even if fault B changes dip in the shallow subsurface, it should reach the surface or deform the alluvial surface somewhere south of Ohio Avenue. Dolan *et al.* (2000) searched extensively for laterally continuous scarps during the study that identified the scarps shown in the figures in our papers. The topographic map from 1934 (Fig. 1), made before regrading of the surface and construction of the courthouse just south of Santa Monica Boulevard, shows the distinct topographic scarp at WVAH but only a smoothly sloping alluvial surface to the south.

Instead of identifying a scarp, Catchings *et al.* drew two arbitrary straight-line slopes on their topographic profile and used these to argue that there is an "inflection point" in the topographic slope near Santa Monica Boulevard with about an "8°" change in slope (Catchings *et al.*, fig. 10 caption). The 8° change in slope they quote was evidently measured directly off the vertically exaggerated profile. The topographic profile in their figure 10 actually shows that the "inflection point" represents a change from about 2.5° to 1.4° of dip after removing the vertical exaggeration (Catchings *et al.* list the vertical exaggeration as being 11:1 in their figure 10, but the actual exaggeration according to the horizontal and vertical scales appears to be about 6.5:1). The topographic profile, however, can be fit almost perfectly by a smooth, concave-up profile typical of alluvial fans (e.g., De Chant, 1999), with the hanging-wall portion of the profile north of the WVAH scarp uplifted several meters (Fig. 1). In other words, the slight, concave-upward slope at Santa Monica Boulevard is entirely consistent with a typical alluvial-fan profile, in contrast to the distinct scarp with a slope of 5° to 6° at the WVAH site. The only unusual topography in the vicinity of Santa Monica Boulevard along our profile is a slightly higher area just south of the roadway, where our seismic profile crossed a man-made, parklike plaza at the west Los Angeles courthouse and public library. There are no laterally continuous features evident on the 1934 topographic map that might be indicative of tectonic activity. The lack of a topographic expression at Santa Monica Boulevard, or anywhere on the alluvial surface south of Ohio Avenue, precludes the possibility that fault strand B, if it exists, has had any recent dip-slip motion on it. The sharp WVAH topographic scarp just north of Ohio Avenue, which is laterally continuous and increases in height to the west, is by far the most pronounced topographic feature in the study area and provides unequivocal evidence for the location of recent faulting. The trench across the scarp confirmed evidence for past earthquakes (Dolan *et al.*, 2000).

Two other pieces of evidence that Catchings *et al.* used to argue for an active fault near Santa Monica Boulevard are inconclusive. First, they used contours of "historically highest groundwater" to argue for a groundwater anomaly near Santa Monica Boulevard (Catchings *et al.*, fig. 7). There is an obvious sampling issue when interpreting this level of detail on the contour map shown in their paper. Specifically, the few wells in the vicinity of the study site have an average spacing of about 600 m, so the contours on the map have few constraints in the study area. Arguing that the contours show evidence for a 200 m difference in the location of the fault is not tenable. As noted previously, the only precisely located groundwater anomalies in the area are along the well-defined topographic scarp that is the westward continuation of the scarp on the WVAH property (at University High and the corner of Wilshire and Bundy; Fig. 1).

Secondly, the Interferometric Synthetic Aperture Radar image showing relative changes in elevation over time is printed at too low a resolution to infer the exact location of active tectonic deformation (Catchings *et al.*, fig. 7b, but the actual positions of the topographic scarps as mapped by Dolan *et al.* (2000) are mislocated on this figure). There is a relatively broad gradient that does not clearly define an inflection point on Catchings *et al.* figure 7b to within a 200 m distance. Perhaps a series of profiles across the anomaly or a more detailed image would be more effective in displaying these data. Certainly, the data as presented in the Catchings *et al.* paper cannot be used to contradict direct observations of recent fault activity in the form of the laterally extensive, well-defined scarp, paleoseismologic observations of recent faulting and folding, and groundwater barriers along the scarp, as well as robust geomorphic negative evidence consisting of the lack of a scarp at the inferred near-surface location of their fault B.

The interpretation by Catchings *et al.* of fault B extending at a shallow angle to north of Wilshire Boulevard is an overinterpretation of our P2 profile and contradicts the subsurface data of Tsutsumi *et al.* (2001). Catchings *et al.* drew short dashed lines on our seismic profile P2 and then used these lines to interpret fault B as extending about 700 m north to beyond Wilshire Boulevard with a dip of about 20° and to a depth of about 450 m (although Catchings *et al.*, fig. 10 actually shows it at less than 300 m depth). We stated in our paper that our "Data quality was marginal…" (p. 483 of Pratt *et al.*, 1998), and we cautiously interpreted only the strongest reflections (see the line drawing in Pratt *et al.*, 1998). We disagree with Catchings *et al.* placing short dashed lines on the deeper parts of our profile, as we feel that doing so is overinterpreting features that more likely are noise.

Borehole data indicate that the active strand of the Santa Monica fault cannot dip at the shallow 20° angle to beneath Wilshire Boulevard, as proposed by Catchings *et al.* This is an important point, as a slip rate calculated from vertical uplift assuming a 20° fault dip would be, for example, more than double that assuming a fault with a 60° dip. In our papers, we added lines to our profile to schematically show the range of possible dip angles for the fault, and we stated that the fault has a steep dip (60° to 70°) that decreases only in the near surface (p. 487 of Pratt *et al.*, 1998; fig. 3 of Dolan *et al.*, 2000). Extending the Santa Monica fault beyond Wilshire Boulevard at about 300 m depth as shown in Catchings *et al.* figure 10, or even at a depth of 450 m as stated in their text, would violate the drill hole data that show the fault at

1.0–1.2 km depth beneath Wilshire Boulevard (Tsutsumi *et al.*, 2001). In fact, the fault must steepen to at least a 60° dip below about 100 m depth if it is to agree with the subsurface data of Tsutsumi *et al.* (2001; see fig. 3 of Dolan *et al.*, 2000).

Catchings *et al.* incorrectly state that "Neither the seismic imaging studies nor trenching studies at WVAH are consistent with the presence of a high-angle reverse fault directly beneath the topographic scarp at WVAH." In both our 1997 and 1998 papers (Dolan and Pratt, 1997; Pratt *et al.*, 1998), we included a figure showing that the "possible dip range" consistent with our data spans from 30° to 55°. We tentatively favored a 30°–35° dip angle based on the possible presence of weak footwall reflectors, but we clearly stated and illustrated that our data permit dip angles as large as 55° for the fault in the upper 200 m.

Unrealistically Fast Velocities in the Catchings *et al.* Velocity Model

The average velocities that Catchings *et al.* presented in their tomographic velocity model below 25 m depth are too fast the shallow Pleistocene alluvium and possibly Plio-Pleistocene (Pico or San Pedro Formation) sedimentary strata imaged in the upper 100 m (Pratt *et al.*, 1998; Tsutsumi *et al.*, 2001). These unrealistically fast velocities bring into question the methodology used to produce the tomographic image, as well as the accuracy of the entire image. The accuracy of the seismic reflection image is also in question because it was derived using the unrealistically fast tomographic velocities. Catchings *et al.* table 4 listed an average velocity of 3600 m/s at depths between 35 and 45 m on the WVAH profile, and their tomographic model had velocities of "4500 m/s within the upper 50 m" (their abstract and their figure 4). These fast velocities are more consistent with deeply buried rocks than with young, shallow sedimentary strata.

The WVAH site overlies young sedimentary strata that form the shallow part of the Los Angeles basin, with Mesozoic basement rocks lying at a depth of 1 km or more (e.g., Tsutsumi *et al.*, 2001). Compilations of velocity measurements in the northern Los Angeles basin show that depth of burial is a key factor for determining seismic velocities (Shaw and Süss, 1998; Süss and Shaw, 2003). Pico Formation and younger rocks are characterized by velocities of 3000 m/s or less at depths above 1 km, and velocities of 4000 m/s are not reached until burial to depths of over 2 km (Fig. 2; Shaw and Süss, 1998). Throughout the Los Angeles Basin, velocities of 4500 m/ sec are not reached in any basin strata until burial to depths of 1 km or more (Fig. 2; Shaw and Süss, 1998; Süss and Shaw, 2003). The Shaw and Süss (1998) and Süss and Shaw (2003) studies include velocity measurements in the northern Los Angeles basin in the vicinity of the WVAH site. The velocities of 3000 to 4500 m/ sec shown in the Catchings *et al.* tomography model at 25 to 50 m depth are much faster than can reasonably be expected for young sedimentary units at such shallow depths (Fig. 2).

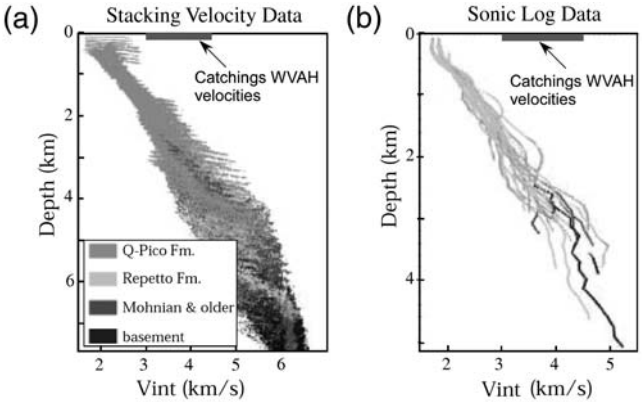

Figure 2. Velocities from the lower part of the Catchings *et al.* tomography image (3000–4500 m/s at 50 m depth or less) compared with compilations of interval velocities from: (a) seismic-reflection stacking velocities in the northern Los Angeles basin; and (b) sonic logs throughout the Los Angeles basin. The WVAH site overlies shallow strata (Pico Formation) that form the upper part of the Los Angeles basin. The 3000–4500 m/s velocities in the lower part of the Catchings *et al.* tomography image are well outside the range of any other velocities determined in the upper 1 km in Los Angeles basin strata. This is a black-and-white version of figure 2 from Shaw and Süss (1998); a similar figure based on seismic travel time is shown as figure 5 in Süss and Shaw (2003).

Velocity measurements made in the 90-m-deep boreholes within 600 m of the seismic profile (and in the Brentwood Veteran's Administration borehole slightly farther north) had average velocities of 1800–2840 m/s and had no velocities interpreted to exceed 2840 m/s (Gibbs *et al.*, 2000; Boore, 2003). Velocities in the northern borehole about 600 m northwest of the seismic profile were interpreted by Gibbs *et al.* (2000) to be 2137 m/s or less to a depth of 90 m, with the exception of a single, 8.6-m thick layer of "Santa Monica slate," with an average velocity of 2840 m/s (Fig. 1). In fact, the "Santa Monica slate" at 38 m depth in the borehole is probably a gravel containing clasts of the true Santa Monica slate (such gravels were observed in the Dolan *et al.* (2000) trench). The sediments at 38 m depth beneath the trench are Pleistocene alluvium, Pleistocene San Pedro Formation, or Plio-Pleistocene Pico Formation. The late Jurassic Santa Monica slate is much lower in the stratigraphic section, with the closest exposures being in the Santa Monica Mountains about 4 km north of the study site (see cross section C-C' in Tsutsumi *et al.* (2001) to see the spatial relationship). If any coherent Santa Monica slate is present beneath the study site, it would be at a depth of 1–1.5 km. In contrast to the borehole velocity measurements, the tomography model of Catchings *et al.* predicts velocities of over 4000 m/s in the lower 35 m of the northern drillhole (dashed yellow line in Catchings *et al.*, fig. 4a). The velocity comparison in Catchings *et al.* table 4 showed that their interpreted WVAH velocities in the 40–50-m borehole-depth range are 39% faster than those measured in the northern borehole (2450 m/s versus 1762 m/s), and the interpreted WVAH velocities in the 50–60-m borehole-depth range are

27% faster than measured borehole velocities (3600 m/s versus 2840 m/s). A comparison of the borehole velocities, the WVAH velocities in Catchings *et al.* table 4, and the velocities from their contours (Catchings *et al.* fig. 4) show the large differences in velocities below 25 m depth (Fig. 3).

Moreover, the northern borehole is located 600 m from the seismic profile, making it unclear whether any of the alluvial-fan deposits (or landslide blocks, if there are any) correlate from the borehole to the seismic profile. The much closer, southern borehole shows even lower velocities. The southern borehole is located about 240 m northeast of the seismic profile, and its location northeast of the seismic profile places it in the hanging wall of the fault rather than in the footwall as interpreted by Catchings *et al.* (their fig. 2). Velocities in this closer borehole were interpreted to be less than 1800 m/s to the bottom of the borehole at a depth of almost 90 m (Gibbs *et al.*, 2000; Catchings *et al.* table 3). In contrast, Catchings *et al.* predicted velocities of over 4000 m/s in the lower 25 m of the southern drillhole (dashed yellow line in Catchings *et al.*, fig. 4a). However, the borehole is closer to the northern end of the seismic profile, where Catchings *et al.* shows velocities of over 4000 m/s at 32 m depth. The high velocities in the lower part of the Catchings *et al.* tomography profile are thus more than double any velocity reported in the nearest borehole.

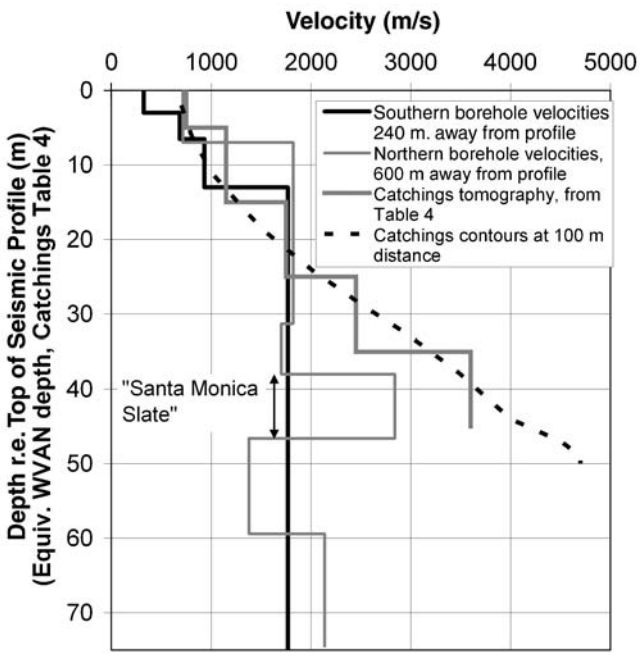

Figure 3. Comparison of velocities in the Catchings *et al.* tomography model with the velocities measured in the WVAH boreholes 600 m north and 240 m northeast of the seismic profile. All depths are relative to the top of the north end of the seismic profile, with the borehole depths of the northern borehole adjusted by −15 m to match the elevation of the seismic profile, as per Catchings *et al.* ("Equivalent WVAN depth" in their table 4). The dotted line shows the average velocities listed in Catchings *et al.* table 4; the heavy dashed line shows the velocities from the contours on the Catchings *et al.* tomography model at distance 100 m. The gray line shows the average velocities interpreted in the northern borehole by Gibbs *et al.* (2000) and also listed by Boore (2003). Velocities in the closest, southern borehole (black line), 240 m northeast of the seismic profile, were less than 1800 m/s for the full 90-m depth of the borehole (Gibbs *et al.*, 2000; Boore, 2003). In contrast, Catchings *et al.* determined velocities as high as 4500 m/s on their tomography image. Below 25 m depth, the velocities listed in Catchings *et al.* table 4 are more than 650 m/s greater than those measured in the northern borehole at the same depth and as much as 1800 m/s greater than any velocity in the southern borehole (3600 m/s versus < 1800 m/s). The 4500 m/s velocities in the Catchings *et al.* profile are more than double any of the borehole velocities except for being only 1.6 times greater than the 2840 m/s "Santa Monica slate" layer.

There is some interpretation in determining the Gibbs *et al.* (2000) borehole velocities, but Boore (2003) stated that the final values were assessed by "a team made up of the seismologists and [the] geologist who logged the hole, as well as other seismologists." The seismic data used to compute velocities in the WVAH boreholes had clear arrivals on both the *P*-wave and *S*-wave records, particularly in the northern borehole that includes the "Santa Monica slate" layer, and the *P*-wave velocities were checked against the *S*-wave velocities by computing Poisson's ratio. Although Gibbs *et al.* (2000) gave lower and upper limits from their inversion as 1700 and 4000 m/s for the "Santa Monica slate," they interpreted the most likely value to be 2840 m/s. The subsequent report by Boore (2003) endorsed the WVAH borehole velocity of 2840 m/s for the "Santa Monica slate," the other velocities of 2137 m/s or lower to 90 m depth in the northern borehole, and the velocities of less than 1800 m/s in the southern borehole. The velocities interpreted by Gibbs *et al.* (2000) and Boore (2003) are consistent with compilations of measured velocities in the Los Angeles basin (e.g., Fig. 2).

Catchings *et al.* used the unrealistically fast velocities from their tomography model to process the seismic reflection image, which brings the accuracy of their reflection image into question. They explicitly state that "…the use of the tomographic velocity data for stacking and migration of the WVAH reflection image are particularly important…" (pp. 133–134), and "…we linearly extended the velocities determined from the tomographic velocity model laterally and vertically in the upper 50 m" (p. 128). Both the stacking and migration processes are sensitive to small errors (~5%–10%) in velocity. Stacking or migrating the seismic reflection data with unrealistically fast velocities could introduce artifacts with the appearance of reflectors and would degrade the imaging of the true reflectors because of inaccurate time corrections. This degradation would be prevalent below about 25 m depth where the velocities used in the processing are unrealistically fast; this depth range includes the entire portion of their profile from which they interpret fault B. The migration process moves reflected energy both horizontally and vertically, so migrating the data using their unrealistically fast imaging velocities could cause the migration process to improperly move deeper energy into the shallower parts of the profile. This makes the upper portion of their profile also suspect, even though their tomographic velocities

are more realistic in the upper 25 m of their image. We used velocities derived from standard seismic reflection velocity analyses to process our data.

Comments on Reflector Geometry

We disagree with the statement Catchings *et al.* made on page 134 that our interpreted fault is inconsistent with our seismic profile because it "would cut the continuous reflections seen on the P2 reflection image above 100-m depth". As best shown in figure 6 of Pratt *et al.* (1998), the continuous shallow reflectors on the P2 profile stop near Ohio Avenue and a 30° or steeper fault reaching the surface at Ohio Avenue does not cut any continuous reflectors on our profile. Pratt *et al.* (1998) also showed that, as the interpreted dip of the fault decreased, the fault tip must reach the surface slightly farther to the south to avoid cutting the shallow reflector at the base of the alluvial-fan deposits. More importantly, our higher-resolution P1 profile, which should provide the better image of the details near the trench, showed the prominent subhorizontal reflectors at 20–40-m depth stopping short of the south end of the trench and north of Ohio Avenue (Catchings *et al.*, figs. 8a and 9a). Finally, if truncation of the reflectors imaged on the P2 profile is a concern, the problem is only exacerbated by the fault A hypothesized by Catchings *et al.*, which approaches the surface about 25–30 m farther north than our interpreted fault. They interpreted fault A to have enough slip to cause a fault-plane reflection (which implies significant motion), to bound a zone of "rotated strata" (Catchings *et al.*, p. 129), and to cause about 10 m of vertical displacement of shallow strata: "…the reflector that correlates best with the 1500 m/sec velocity contour increases in depth from about 5 m north of fault A to about 15 m south of the surface projection of fault A" (p. 131; see also Catchings *et al.*, figure 6b). If there is not significant dip-slip motion on their fault A, then they provide no explanation for the presence of the fault scarp and the folded strata evident within the trench, for the tomographic velocity change beneath the south end of the trench, or for the groundwater anomaly (springs) coincident with the scarp.

Catchings *et al.* also questioned the validity of subhorizontal reflectors we imaged below 20 m depth on the north half of our profile P1 (their figure 8a; text on pp. 132–133), arguing that the shallow strata dip slightly southward. In contrast, their profile has reflections that suggest that strata dip to the south at angles as great as 25° in the 15–50 m depth range from the north side to the center of their profile (their fig. 5a, b). Subhorizontal reflectors are supported by other geophysical and geological observations: (1) the water table should be a relatively flat reflector (the interface is sometimes reflective); (2) the alluvial strata exposed in the trench and the fan surface north of the scarp dip southward at angles of less than 3°; and (3) Catchings *et al.* showed a nearly horizontal layer of "Santa Monica slate" at a depth of about 38 m (Catchings *et al.*, fig. 6b). If the contours on their velocity model are representative of the underlying geology, they indicate effectively flat strata on the north half of their profile (Catchings *et al.*, fig. 4a). Their interpretive geologic model (Catchings *et al.*, fig. 6b) implied or explicitly showed predominantly subhorizontal layers to 50 m depth, consistent with the subhorizontal reflections on our seismic profile (compare Catchings *et al.* figs. 6b and 8a). In contrast, a distinct subhorizontal reflection from the top of their interpreted high-velocity "Santa Monica slate" layer is notably absent on the Catchings *et al.* profile, the right half of which is dominated by apparent reflections that dip to the south at far greater dips (up to 25°) than any strata interpreted in the immediate area (their fig. 5a,b).

Summary

The preponderance of the evidence reviewed here suggests that nearly all of the ~180 m of apparent vertical displacement on the Santa Monica fault in the WVAH study area is on a fault that approaches the surface near Ohio Avenue immediately south of the trench and laterally continuous topographic scarp, as we interpreted in our earlier papers (shown in Catchings *et al.*, fig. 9a). Catchings *et al.* fault B, if it exists, cannot be the active, near-surface strand of the Santa Monica fault. The topographic profile in Catchings *et al.* and the topographic map we present here demonstrate that there is no scarp south of Ohio Avenue, including where their fault B was hypothesized to reach the surface near Santa Monica Boulevard, but rather a smoothly concave-up topographic profile typical of alluvial fans (Figure 1). Fault B described by Catchings *et al.* also lies too far south to cause the velocity anomaly seen on the Catchings *et al.* tomography profile and the groundwater anomalies at the WVAH topographic scarp. The Santa Monica fault also must have a steeper dip than the Catchings *et al.* fault B if it is to honor the subsurface data in Tsutsumi *et al.* (2001). Catchings *et al.* fault A cannot have the ~10 m of recent vertical displacement that they infer because it does not displace the strata excavated in the trench. Thus, neither of the faults interpreted by Catchings *et al.*, if they exist, can be the main strand of the Santa Monica fault that caused the folding of strata within the trench and generated the well-defined, laterally continuous topographic scarp. The active strand of the Santa Monica fault near WVAH must lie just south of the topographic scarp, at the base of the folded strata excavated in the trench, as we interpreted in our earlier papers.

Data and Resources

The data in this paper have been presented in previous publications listed in the references.

Acknowledgments

We thank William Stephenson, Patricia McCrory, and Thomas Brocher of the U.S. Geological Survey (USGS) and John Shaw of Harvard University for comments that improved the manuscript.

References

Boore, D. M. (2003). A compendium of *P*- and *S*-wave velocities from surface-to-borehole logging: Summary and reanalysis of previously published data and analysis of unpublished data, *U.S. Geological Survey Open-File Report 03 -191*, 13 p. plus electronic database.

Catchings, R. D., G. Gandhok, M. R. Goldman, D. Okaya, M. J. Rymer, and G. W. Bawden (2008). Near-surface location, geometry, and velocities of the Santa Monica fault zone, Los Angeles, California, *Bull. Seismol. Soc. Am.* **98,** 124–128. doi 10.1785/0120020231.

De Chant, L. J., P. P. Pease, and V. P. Tchakerian (1999). Modelling alluvial fan morphology, *Earth Surf. Processes Landforms* **24,** 641–652.

Dolan, J. F., and T. L. Pratt (1997). High-resolution seismic reflection profiling of the Santa Monica fault zone, west Los Angeles, California, *Geophys. Res. Lett.* **24,** 2051–2054.

Dolan, J. F., K. Sieh, and T. K. Rockwell (2000). Late Quaternary activity and seismic potential of the Santa Monica fault system, Los Angeles, California, *Geol. Soc. Am. Bull.* **112,** 1559–1581.

Gibbs, J. F., J. C. Tinsley, D. M. Boore, and W. B. Joyner (2000). Borehole velocity measurements and geological conditions at thirteen sites in the Los Angeles, California region, *U.S. Geol. Surv. Open-File Rept. 00-470*, 118 pp.

Hill, R. L. (1979). Potrero Canyon fault and University High School escarpment, in *Field Guide to Selected Engineering and Geologic Features, Santa Monica Mountains*, J. R. Keaton, Chairman, Association of Engineering Geologists, Southern California Section, Annual Field Trip Guide, 83–103.

Hill, R. L., E. C. Sprotte, J. H. Bennett, C. R. Real, and R. C. Slade (1979). Location and activity of the Santa Monica fault, Beverly Hills-Hollywood area, California, in *Earthquake Hazards Associated with Faults in the Greater Los Angeles Metropolitan Area, Los Angeles County, Including Faults in the Santa Monica-Raymond, Verdugo-Eagle Rock, and Benedict Canyon Fault Zones*, *Calif. Div. Mines and Geol. Open-File 79-16 LA*, B1-B43.

Pratt, T. L., J. F. Dolan, J. K. Odum, W. J. Stephenson, R. A. Williams, and M. E. Templeton (1998). Multiscale seismic imaging of active fault zones for hazard assessment: A case study of the Santa Monica fault zone, Los Angeles, California, *Geophysics* **63,** 479–489.

Shaw, J. H., and M. P. Süss (1998). Velocity structure of the Los Angeles basin from sonic logs and stacking velocities, Southern California Earthquake Center Annual Report, 1998, available at http://www.scec.org/research/98research/98shawsuss.pdf (last accessed June 2010).

Süss, M. P., and J. H. Shaw (2003). *P* wave seismic velocity structure derived from sonic logs and industry reflection data in the Los Angeles basin, California, *J. Geophys. Res.* **108,** 2170. doi 10.1029/2001JB001628.

Tsutsumi, H., R. S. Yeats, and G. J. Huftile (2001). Late Cenozoic tectonics of the northern Los Angeles fault system, California, *Geol. Soc. Am. Bull.* **113,** 454–468.

U.S. Geological Survey
School of Oceanography
Box 357940
University of Washington
Seattle, Washington 98195
tpratt@ocean.washington.edu
(T.L.P.)

Department of Earth Sciences
University of Southern California
Los Angeles, California
90089-0740
dolan@usc.edu
(J.F.D.)

Manuscript received 8 June 2009